Cluster Statistics and Traffic on a Lattice

Thorsten Pöschel and Jan A. Freund

Institute of Physics, Humboldt–University, Invalidenstr. 110, D–10115 Berlin, Germany

Abstract. We describe traffic on a two dimensional lattice modelled using a cellular automaton. The theoretical approach valid in the low density region employs cluster statistics. The derived central formula for the velocity vs. density relation nicely agrees with simulation results. In our approach the explicit traffic rules solely enter through combinatorics accounting for average crossing traffics.

1 Introduction

Traffic phenomena have been analyzed employing various approaches including hydrodynamic descriptions, kinematic waves, cellular automata and others (for a commented compilation of references see Freund and Pöschel 1995). A crucial feature of traffic systems is a collapse of the average traffic flow when the car density exceeds a critical value. This jamming transition is not only observed in real traffic systems but is also reflected by many one– and two–dimensional models.

In this article we consider traffic on a two–dimensional lattice with periodic boundary conditions (see fig. 1). Each lattice site represents a crossing of four queues each of which can be occupied by at most Q cars. Employing cluster analysis we will provide an approximation for the average car velocity as a function of the global car density.

2 Description of the System

Henceforth, the number of cars will be denoted by N, the number of lattice sites by $M = L \times L$, and the global car density by $\eta = N/M$.

In each time step cars waiting at the top position of a queue can move to a neighbouring site, i.e. a site being located either to the left, to the right, or ahead of the present one. However, in case it has to give way obeying a certain set of traffic rules it remains waiting. Cars queueing behind the top position move one position forward if its place ahead is empty. In our description there exist only two velocities, namely $v = 1$ for cars moving to a next site and $v = 0$ for all others, respectively.

Denoting the total number of cars prevented from moving in a given time step t by $\mathit{\Delta}(t)$ the central quantity is the time averaged global car velocity

$$\overline{v} = \frac{1}{T}\sum_{t=1}^{T}\frac{N-\mathit{\Delta}(t)}{N} = 1 - \frac{\langle \mathit{\Delta}\rangle_T}{N}\ . \qquad (1)$$

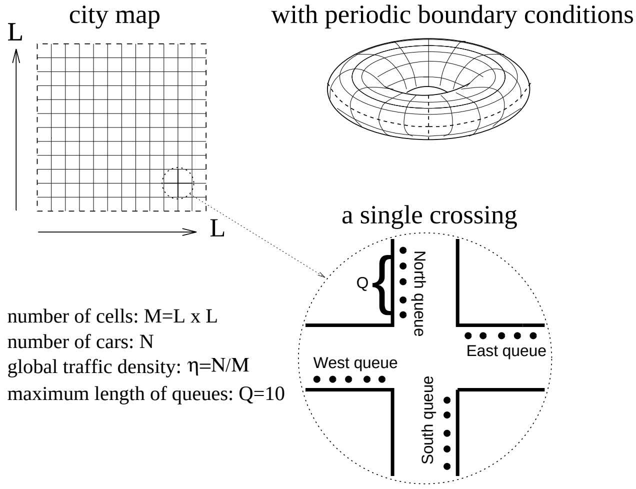

Fig. 1. Draft of the investigated street network on an $L \times L$ lattice with periodic boundary conditions.

Here, T has to be chosen sufficiently large in order to scan the state space resp. the limit set with sufficient accuracy.

For very small car density, i.e. for $N \ll M$, it is obvious that $\langle \Delta \rangle_T \ll 1$ since cars rarely meet, yielding $\overline{v} \lesssim 1$. With increasing car density η the probability of cars to meet rises, hence, $\langle \Delta \rangle_T$ grows resulting in a decline of $\overline{v}$.

3 Cluster Statistics Approach

Our mathematical approach essentially is based on two assumptions:

1. The dynamics can be separated into the global process of clustering and the local process of updating the crossings with respect to the traffic rules. In this context, any configuration of k cars meeting at a site is regarded as a cluster of size k.
2. The dynamics generates cluster distributions and crossing configurations without any temporal correlations. Thus, the temporal statistics may equivalently be represented by ensemble statistics.

The long–time statistics is characterized by a probability of cluster configurations $\underline{k} = (k_0, k_1, \ldots, k_{4Q})$ where $0 \leq k_i \leq M$ denotes the number of clusters of size i. Valid configurations have to obey two boundary conditions, namely

$$\sum_{i=0}^{N} k_i = M \qquad \text{and} \qquad \sum_{i=0}^{N} i k_i = N \ . \tag{2}$$

Under the aforementioned assumptions the temporal cluster statistics is accessible through combinatorial reasoning. The probability of a valid cluster configuration reads

$$p(\underline{k}) \ = \ \frac{M!\ N!}{M^N \prod_{j=0}^{N} \left[(j!)^{k_j}\ k_j!\right]} \ . \tag{3}$$

To understand formula (3) in detail one has to realize that there exist $M!/\left[k_0!k_1!\ldots k_N!\right]$ different ways to index M cells with numbers $0,1,\ldots,N$ since all cells containing the same number i of cars are not distinguishable. Then there exist $N!/\left[(0!)^{k_0}(1!)^{k_1}\ldots(N!)^{k_N}\right]$ ways to index the cars with numbers $1,\ldots,N$ taking care of the fact that cars within the same cell are not distinguishable. Finally, the equidistribution with respect to all configurations yields the factor M^{-N}. This result was first obtained by von Mises (1939).

Now the time average $\langle \Delta \rangle_T$ occurring in (1) is replaced by the ensemble average

$$\langle \Delta \rangle_{\underline{K}} \ = \ \sum_{\underline{k}}^{*} p(\underline{k}) \sum_{i=1}^{N} k_i \overline{\delta_i}\, \alpha_i \ . \tag{4}$$

The sum with respect to all configurations obeying (2) – which is indicated by the symbol $*$ – accounts for the cluster statistics. The factor α_i reflects the fact that the dynamics of the real process slightly differs from a Bernoulli–process. They can be found by considering recurrence paths (Freund and Pöschel 1995).

The δ_i reflect the average delay due to the traffic rules at the crossings. Note that it is here and only here that explicit traffic rules enter our approach. The calculation of the δ_i requires combinatorial considerations. Obviously the number δ_i is confined to the interval $[0,i]$. The average is performed with respect to all possible configurations which are assumed to occur with equal probability. The case $i=1$ is rather simple: If there is only one car at the crossing it never has to give way hence, $\overline{\delta_1}=0$. The case $i=2$ is not that trivial and the computation of $\overline{\delta_2}$ requires some combinatorial effort. Since each of the cars can wait at one of the four sides of the crossing and can proceed in one of the three directions (left, straight on, right) we have $4\times 3\times 4\times 3=144$ different situations of equal probability. Each of these situations can be assigned to one of the situations in the left column of table 1. We now explain the columns of table 1:

1. A sketch of the configuration given by a graph.

Table 1. All situations which might occur when two cars meet at a crossing, their frequency, their symmetry according to rotation and due to indistinguishability of the cars and the number of cars which have to stop in the current situation (explanation in the text).

graph	rot. symm.	dist.	#events	waiting	#stopping
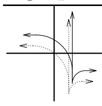	$4 \times 3 \times 3$	1	36	1	36
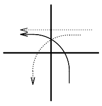	$4 \times 1 \times 2$	2	16	1	16
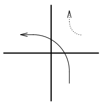	$4 \times 1 \times 1$	2	8	0	0
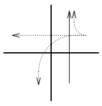	$4 \times 1 \times 3$	2	24	1	24
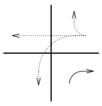	$4 \times 1 \times 3$	2	24	0	0
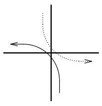	$2 \times 1 \times 1$	2	4	0	0
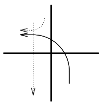	$4 \times 1 \times 2$	2	16	1	16
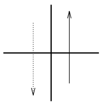	$2 \times 1 \times 1$	2	4	0	0
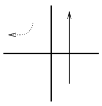	$4 \times 1 \times 1$	2	8	0	0
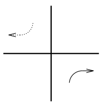	$2 \times 1 \times 1$	2	4	0	0
	total		144		92

Table 2. The average number of cars which are stopped $\overline{\delta_i}$ when i cars meet at a crossing.

#cars meeting i	$\overline{\delta_i}$
1	0.0
2	0.638889
3	1.479167
4	2.467014
5	3.524740
6	4.604709
7	5.683838
8	6.752964

2. The number of the different realizations that relate to the graph in the first column assuming first that the cars are distinguishable. The first factor A in the form $A \times B \times C$ originates from the symmetry according to rotation by $\frac{1}{2}\pi$, π and $\frac{3}{2}\pi$. The second factor B denotes the number of choices for the first car (which is now assumed to come from South) and the last factor C gives the number of situations possible for the second car.
3. When we take into account that the cars in fact cannot be distinguished the number of different events that belong to the figure in the first column has to be multiplied by the factor given in the third column.
4. The total number of events for the whole class denoted by the graph, i.e. (column 2$\times$ column 3).
5. The number of cars stopped by the traffic rules at this crossing in one of the possible realizations (either one or none).
6. The total number of cars which have to stop related to the whole class denoted by the graph, i.e. (column 4$\times$ column 5).

From the last line in table 1 one sees that there are 144 different situations of equal probability which amounts to 288 cars. Furthermore, we see that 92 of those 288 cars have to stop. Hence, the average number of the cars stopped for 2–clusters is $\overline{\delta_2} = 92/144 \approx 0.639$.

For the clusters of size $i = 3$ the average number of cars which are prevented from moving $\overline{\delta_3}$ can be calculated in analogy however the corresponding table contains about 8 times as much situations as table 1. Therefore we do not want to present it here. The result is $\overline{\delta_3} = 1.479$. For cluster of size larger than 3 the corresponding $\overline{\delta_i}$ have been calculated by the method of complete enumeration using a computer. These empirical results are collected in table 2. For $i = 1 \dots 3$ they are identical with the analytical results.

For completeness sake we remark that for large cluster sizes ($i > 8$) there exists a negligible probability that one of the directions of the crossing is not occupied. Typically there are many cars waiting in each of the four queues. In those very likely cases our traffic rules allow exactly one (randomly chosen) cars to drive, all other $i-1$ cars have to stop. Therefore we find $\overline{\delta_i} \stackrel{i \gg 1}{\rightarrow} i-1$. Certainly the contributions of such big clusters will only play a minor role in our calculations due to very small likelihood.

Inserting expression eq.(4) into (1) yields

$$\overline{v} = 1 - \frac{\langle \Delta \rangle_{\underline{K}}}{N} = 1 - \sum_{i=1}^{N} \frac{\overline{\delta_i} \alpha_i}{N} \sum_{k_1,\ldots,k_N}^{*} k_i \, p(k_1,\ldots,k_N) \tag{5}$$

and performing the sum over all k_j ($j \neq i$) we find

$$\begin{aligned} \overline{v} &= 1 - \sum_{i=1}^{N} \frac{\overline{\delta_i} \alpha_i}{N} \sum_{k_i=0}^{\lfloor N/i \rfloor} k_i \, p(k_i) \\ &= 1 - \sum_{i=1}^{N} \frac{\overline{\delta_i} \alpha_i}{N} \, \langle K_i \rangle \, . \end{aligned} \tag{6}$$

The distribution $p(k_i)$ – declared for $i = 0, 1, \ldots, \lfloor N/i \rfloor$ – can be calculated using the inclusion–exclusion principle (Johnson and Kotz 1977, Krengel 1990). Note that the problem to find $p\,(k_i)$ is different from the trivial problem to find the probability for the k_i crossings which are occupied by *at least* i cars.

The inclusion–exclusion principle relates the probabilities for a finite number of sections of events to the probabilities of an exact number of events.

Let (Ω, P) be a probability space, $A_1, \ldots, A_N$ be events, and for arbitrary $\{m_1, \ldots, m_j\} \subset \{1, \ldots, N\}$ let $P(A_{m_1} \cap \ldots \cap A_{m_j})$ be known probabilities. We define

$$S_j = \sum_{m_1,\ldots,m_j} P(A_{m_1} \cap \ldots \cap A_{m_j}) \tag{7}$$

Moreover, let be $B_n = \{\omega \in \Omega : \omega \in A_m \text{ for exactly } n \text{ values of } k\}$. Then the inclusion–exclusion principle asserts that

$$P(B_n) = \sum_{j=n}^{N} (-1)^{(j-n)} \binom{j}{n} S_j \tag{8}$$

Applied to our case the S_j are the probabilities that j cells each contain i cars and the rest of the cars, i.e. $(N - ji)$ cars, are distributed arbitrarily among the remaining $(M - j)$ cells; this probability can be derived with ease and reads

$$S_j = \frac{N!}{(i!)^j \, (N-ji)!} \left(\frac{1}{M}\right)^{(ji)} \left(1 - \frac{j}{M}\right)^{(N-ji)} \tag{9}$$

To explain this formula we first index each of the N cars with the numbers $1, \ldots, N$ which yields the factor $N!$. Since the i cars within each of the j cells are not distinguishable we have to divide this factor by $(i!)^j$ and since the remaining $(N - ji)$ cars are not distinguishable too additionally by $(N - ji)!$. After having numbered the cars we subsequently fill the first cell with cars $1, \ldots, i$, the second cell with cars $(i + 1), \ldots, (2i)$ and so on. In this way we distribute the cars numbers $1, \ldots, ji$ among the urns $1, \ldots, j$ yielding the factor $M^{(-ji)}$. The remaining $(N - ji)$ cars are distributed successively among the remaining $M - j$ cells at random which explains the factor $[(M - j)/M]^{(N-ji)}$.

Insertion of this probability into the inclusion–exclusion formula (8) yields

$$\begin{aligned} p(k_i) &= \sum_{j=k_i}^{M} (-1)^{(j-k_i)} \binom{j}{k_i} S_j \\ &= \frac{N!}{M^N} \sum_{j=k_i}^{M} (-1)^{(j-k_i)} \binom{j}{k_i} \frac{(M-j)^{(N-ji)}}{(i!)^j \; (N-ji)!} \; . \end{aligned} \tag{10}$$

Because of the generalized definition of factorials – using the gamma function – the sum effectively only ranges from k_i up to $\lfloor M/i \rfloor$ which is sensible.

We see from (6) that the ingredients we actually need are the first moments $\langle K_i \rangle$ of the cluster distribution. They can be derived calculating a generating function for the (descending factorial) moments, denoted $H_i^{(M)}(z, x)$ (Johnson and Kotz 1977)

$$H_i^{(M)}(z,x) = \sum_{N=0}^{\infty} \sum_{k_i=0}^{\infty} \frac{M^N z^N}{N!} \, x^{k_i} \, p(k_i, N) \tag{11}$$

where $p(k_i, N)$ is the probability to find a value k_i for the stochastic variable K_i when trying with N cars. The benefit of such a complicated looking generating function is that the sums can be performed yielding an analytical expression namely

$$H_i^{(M)}(z,x) = \left[\exp^z + \frac{z^i}{i!}(x-1)\right]^M \tag{12}$$

For the explicit derivation the reader is referred to the book by Johnson and Kotz[1] p. 116ff (Johnson and Kotz 1977). Moreover, this function is related to the (descending) factorial moments of the stochastic variable K_i according to

$$\frac{N!}{M^N} \; \frac{d^r}{dx^r} \; \left(H_i^{(M)}(x,z) \right|_{x=1}$$

[1] one has to identify $j \equiv i, m \equiv M, n, \equiv N, M_i \equiv K_i, g \equiv k_i, \Pr[M_j = g|n] \equiv p(k_i)$

$$= \sum_{N=0}^{\infty} z^N \sum_{k_i=0}^{\infty} k_i\,(k_i-1)\,\ldots(\,k_i-r+1)\,p(k_i,N)$$

$$= \sum_{N=0}^{\infty} z^N \,\Big\langle k_i(k_i-1)\ldots\,(k_i-r+1)\Big\rangle \tag{13}$$

hence, the first moment $\langle K_i \rangle$ is given as the coefficient of z^N in

$$\frac{N!}{M^N}\,\frac{d}{dx}\left(H_i^{(M)}(z,x)\right|_{x=1} \tag{14}$$

Consequently, we calculate

$$\begin{aligned} \frac{N!}{M^N}\ \ \frac{d}{dx}&\left(\left[\exp^z + \frac{z^i}{i!}(x-1)\right]^M\right|_{x=1} \\ &= \frac{N!}{M^{(N-1)}}\ \exp^{[z(M-1)]}\ \frac{z^i}{i!} \\ &= \sum_{k=0}^{\infty} \frac{N!}{i!\;k!}\ \frac{(M-1)^k}{M^{(N-1)}}\ z^{(k+i)} \end{aligned} \tag{15}$$

and finally arrive at

$$\begin{aligned} \langle K_i \rangle &= \frac{N!}{i!\;(N-i)!}\ \frac{(M-1)^{(N-i)}}{M^{(N-1)}} \\ &= \binom{N}{i}\ \frac{1}{M^{(i-1)}}\ \left(1-\frac{1}{M}\right)^{(N-i)} \quad . \end{aligned} \tag{16}$$

In fig. 2 we have depicted the expectation value of the cluster distribution $\langle K_i \rangle$ (eq. (16)) divided by the system size $M = L \times L$. The solid lines correspond to the function given in eq. (16) and the points represent related data taken from a simulation on a 50×50 torus. The values for $i = 0$ give the probability for a site to be empty. For $i = 0$ and $i = 1$ the analytical and numerical results perfectly agree, for larger i the discrepancies between the solid lines and points are a direct consequence of deviations from the assumed independent behavior as explained in (Freund and Pöschel 1995). Note that the probabilities in fig. 2 are plotted using a logarithmic scale. The observed discrepancies for clusters of size larger than 3 will hardly have any influence on the overall behavior of the automaton. For values $\eta > \eta_{cr}$ the simulation data illustrate a breakdown for the small occupation numbers (except $i = 0$) due to the emergence of jams which are clusters of high order. At the transition point the occupation rates abruptly drop by three orders of magnitude. The precise position of this transition point is masked by the finite size of N used in the simulation. Increasing the car density η beyond the blurred critical zone results in a slow rise of the occupation number for the small

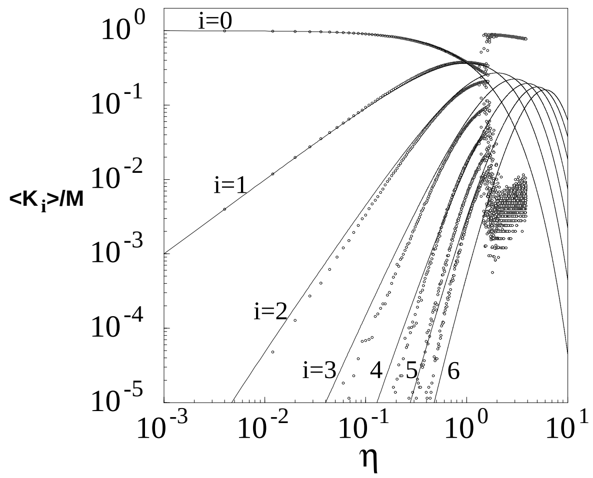

Fig. 2. The average number of clusters of size i normalized to the lattice size $M = L \times L$ as a function of the global traffic density $\eta = N/M$. The lines represent eq. (16) while the points correspond to numerical data achieved by a simulation on a 50×50 lattice (torus). The curve $i = 0$ gives the probability for a site to be empty.

clusters and simultaneously, in a slow decline of the number of empty sites. This is due to the increasing number of cars still moving around the jammed crossings.

Inserting equation (16) into (6) yields the following formula

$$\overline{v} = 1 - \sum_{i=1}^{N} \frac{\overline{\delta_i}\alpha_i}{N} \binom{N}{i} \frac{1}{M^{(i-1)}} \left(1 - \frac{1}{M}\right)^{(N-i)} . \tag{17}$$

The last step will be to substitute in (17) the density η for the number of cars according to $N = \eta M$ which results in

$$\overline{v} = 1 - \sum_{i=1}^{\eta M} \frac{\overline{\delta_i}\alpha_i}{i!} \left(\eta - \frac{1}{M}\right) \cdot \ldots \cdot \left(\eta - \frac{i-1}{M}\right) \left(1 - \frac{1}{M}\right)^{(\eta M - i)} \tag{18}$$

The main result of our statistical description, namely the mean velocity as a function of the car density (eq. (18)), is plotted in fig. 3. The solid line shows the function given by eq. (18) and the points are the data taken from the simulation on a 50×50 torus. In the low density region we find a nice agreement. The closer one approaches the transition point the more eq. (18)

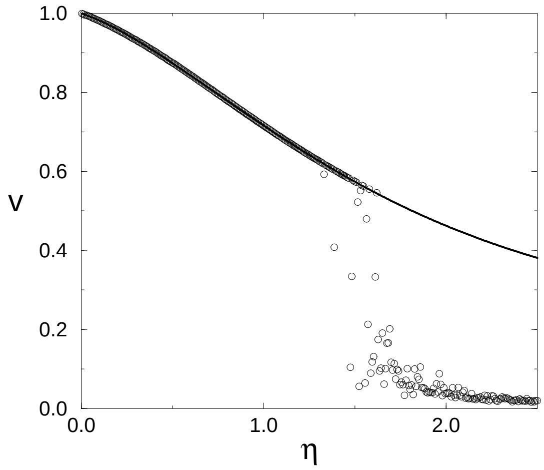

Fig. 3. The average velocity vs the global traffic density for the low density regime (non jamming traffic). The curve displays the result from equation (18), the points show data taken from the simulation.

overestimates the simulation results. This can be understood by recalling the fact that for densities close to the critical value the effective decomposition of the automaton dynamics into the cluster dynamics and the single site dynamics becomes inappropriate due to formation and dissolution of short lived jams (like critical fluctuations). They tend to increase the occupation number of larger clusters and hence, lead to an effective decrease of the average velocity.

In the thermodynamic limit – which means $M, N \to \infty$ and keeping $\eta = N/M$ constant – we drop terms of order $\mathcal{O}(M^{-1})$ and end up with

$$\overline{v} \stackrel{M\to\infty}{\approx} 1 - \sum_{i=1}^{\eta M} \frac{\overline{\delta_i}\alpha_i}{i!}\, \eta^{(i-1)}\, \exp(-\eta) \tag{19}$$

where the exponential corresponds to the dominant contribution of the last factor in (18). This formula can be expressed by a series expansion in powers of η

$$\begin{aligned} \overline{v} \stackrel{M\to\infty}{\approx} &\ 1 - \sum_{i=1}^{\eta M} \sum_{k=0}^{\infty} \frac{(-1)^k \overline{\delta_i}\alpha_i}{i!k!}\, \eta^{(i-1+k)} \\ = &\ 1 - \left(\frac{\overline{\delta_2}\alpha_2}{2}\right)\eta + \left(\frac{\overline{\delta_2}\alpha_2}{2} - \frac{\overline{\delta_3}\alpha_3}{6}\right)\eta^2 \\ &- \left(\frac{\overline{\delta_2}\alpha_2}{4} - \frac{\overline{\delta_3}\alpha_3}{6} + \frac{\overline{\delta_4}\alpha_4}{24}\right)\eta^3 + - \ldots \end{aligned} \tag{20}$$

Note that there is no constant term in the double sum since $\overline{\delta_1} = 0$. Equation (20) can be truncated at a given order of η hence, giving rise to an approximation scheme. In fig. 4 we plotted the linear (dashed), the quadratic (dotted) and cubic (long dashed) approximations together with the full formula (fat solid). The range of reliability visibly increases with increasing the

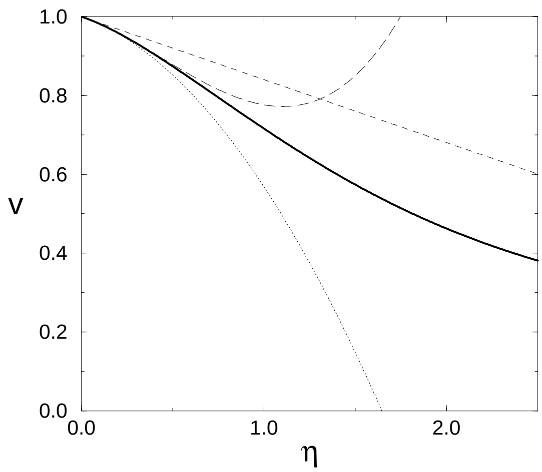

Fig. 4. The average velocity as derived from the statistical description (eq. (16)) (fat line) and truncated series expansions: linear (dashed), quadratic (dotted) and cubic (long dashed). This plot clearly illustrates a nonlinear relationship between average velocity and global density.

order of approximation. On the other hand this scheme clearly illustrates that the functional relation between mean velocity and global density definitely is *nonlinear*, except for very small car densities. This result is in contradiction with earlier results by Martínez et al. Martinez *et al.* 1995.

4 Conclusion

We investigated the behavior of a two–dimensional cellular automaton with periodic boundary conditions to simulate traffic flow in cities. The automaton mimics realistic traffic rules which apply to our everyday experience of vehicular traffic. In agreement with similar models we found a slow decay for the mean velocity $\langle v \rangle$ as a function of the global traffic density η. At a critical threshold value η_{cr} the mean velocity collapses abruptly and the system transits into another regime of global behavior which we call the jamming regime. Beyond the critical density η_{cr} the average velocity is very small and it declines further when increasing the density. By simulating different sizes of automata we could exclude the influence of finite size effect provided the density value is not rather close to the critical density.

Applying combinatorics and statistical methods for the description of the system in the low density regime the analytical calculation performed in sec. 3 yielded the average car velocity as a function of the car density – $\langle \overline{v} \rangle (\eta)$ – which nicely agrees with the values of numerical simulations. Since the derived functional relationship between mean velocity and global traffic density was based on very general assumptions (conservation of the number of cars, weak spatial correlations in the low density regime, ergodicity) we expect this description to be valid for a wider class of traffic systems. Note that the specific structure of traffic rules enters the description only through the average delays δ_i. The only nonlocal ingredient arises from the restriction that cars have to stop in case the next desired queue at a neighboring site is totally filled up. But this nonlocal character only becomes substantial for densities close to the critical value where it causes long range spatial correlations.

Several authors (e.g. Martinez *et al.* 1995) assert that the average velocity $\overline{v}$ in the low density regime is a linear function of the density η and indeed the simulation results seem to support this observation. A more detailed analysis however reveals that this function definitely is nonlinear. An analytic expansion shows (eq. (20), fig. 4) that the results become dramatically wrong when truncating the formula after the linear term. Surprisingly the analytic description gives good results even for densities not too small where the nonlocal effects of the dynamics and hence, long range correlations spoil the basic assumptions of our treatment.

For still higher values of the density η the results of our simulation agree with results reported in literature (e.g. Martinez *et al.* 1995 and many others), but no longer with our approximate theory. Above a critical density we observe an abrupt transition of the system into the jammed regime where the averaged velocity is close to zero. This regime however is beyond the scope of our statistical description and has to be investigated starting from other approaches (e.g. nucleation processes).

We thank U. Küchler for helpful discussion.

References

Freund, J., Pöschel, T. (1995): Physica A **219**, 95.

v. Mises, R. (1939) *Rev. Fac. Sci. Univ. Istanbul* **4**, 145. reprinted in *Selected Papers of Richard von Mises*, Vol. 2. Providence, R.I.: American Mathematical Society, 313 (1964).

Johnson J. N., Kotz, S. (1977): *Urn Models and Their Application*, Wiley & Sons, New York, London, Sydney, Toronto.

Krengel, U. (1990): *Einführung in die Wahrscheinlichkeitstheorie und Statistik*, Vieweg Verlag, Braunschweig, second edition.

Martínez, F. C., Cuesta, J., Molera, J. M., and Brito, R. (1995): Phys. Rev. E **51**, R835.